OAK RIDGE NATIONAL LABORATORY LIBRARIES
3 4456 0549197 3

CENTRAL RESEARCH LIBRARY
DOCUMENT COLLECTION

OAK RIDGE NATIONAL LABORATORY
operated by
UNION CARBIDE CORPORATION
NUCLEAR DIVISION
for the
U.S. ATOMIC ENERGY COMMISSION

UNION CARBIDE

ORNL-TM-1515

1

Talk Bloom McCoy about this

POSTIRRADIATION CREEP AND STRESS RUPTURE OF HASTELLOY N

W. R. Martin
J. R. Weir

CENTRAL RESEARCH LIBRARY
DOCUMENT COLLECTION
LIBRARY LOAN COPY
DO NOT TRANSFER TO ANOTHER PERSON
If you wish someone else to see this document, send in name with document and the library will arrange a loan.

NOTICE This document contains information of a preliminary nature and was prepared primarily for internal use at the Oak Ridge National Laboratory. It is subject to revision or correction and therefore does not represent a final report.

LEGAL NOTICE

This report was prepared as an account of Government sponsored work. Neither the United States, nor the Commission, nor any person acting on behalf of the Commission:

A. Makes any warranty or representation, expressed or implied, with respect to the accuracy, completeness, or usefulness of the information contained in this report, or that the use of any information, apparatus, method, or process disclosed in this report may not infringe privately owned rights; or

B. Assumes any liabilities with respect to the use of, or for damages resulting from the use of any information, apparatus, method, or process disclosed in this report.

As used in the above, "person acting on behalf of the Commission" includes any employee or contractor of the Commission, or employee of such contractor, to the extent that such employee or contractor of the Commission, or employee of such contractor prepares, disseminates, or provides access to, any information pursuant to his employment or contract with the Commission, or his employment with such contractor.

ORNL-TM-1515

Contract No. W-7405-eng-26

METALS AND CERAMICS DIVISION

POSTIRRADIATION CREEP AND STRESS RUPTURE OF HASTELLOY N

W. R. Martin and J. R. Weir

Submitted to Nuclear Applications

JUNE 1966

OAK RIDGE NATIONAL LABORATORY
Oak Ridge, Tennessee
operated by
UNION CARBIDE CORPORATION
for the
U.S. ATOMIC ENERGY COMMISSION

OAK RIDGE NATIONAL LABORATORY LIBRARIES
3 4456 0549197 3

CONTENTS

	Page
Abstract	1
Introduction	2
Experimental	3
Postirradiation Creep and Stress-Rupture Results	3
Conclusions and Summary	27
Acknowledgments	28
References	29

ABSTRACT

The creep ductilities of irradiated Hastelloy N at 650°C have been determined at several neutron exposures. Elevated-temperature irradiation embrittlement greatly reduces the stress-rupture strength as measured in postirradiation uniaxial stress tests. The reduction in ductility to values as low as 0.4% is due to an irradiation effect related to the process of intergranular fracture. Intergranular cracks, once formed, propagate with greater ease in the irradiated alloy as compared with a sample exposed to a lesser radiation exposure.

INTRODUCTION

Iron- and nickel-base alloys are widely used as structural materials in the nuclear industry. Stainless steels and Inconel-type alloys are materials common to nuclear power reactors. The alloy Hastelloy N, which was developed for its resistance to corrosion in molten-salt environments at elevated temperatures, is also of interest because of its high strength in the temperature range 500 to 700°C.

The use of nickel- and iron-base alloys in neutron environments at these elevated temperatures results in irradiation embrittlement in these alloys. The Hastelloy N alloy is no exception, and the embrittlement of this alloy has been discussed previously.[1] This elevated-temperature embrittlement is unlike the fast-neutron displacement whose characteristics have been studied for years. The irradiation damage in the creep range has been generally attributed[2,3,4] to the (n,α) reactions producing helium, which affects the process of intergranular fracture. Most of the helium generated comes from the $^{10}B(n,\alpha)$ reaction with neutrons in the thermal energy range. However, in the absence of either ^{10}B or thermal neutrons, helium can be generated from (n,α) reactions between iron, nickel, nitrogen, etc., with neutrons in high energy range.[5,6]

The degree of embrittlement has been primarily measured by conducting postirradiation tensile tests,[7,8] in-reactor tube-

burst tests,[2,9] and postirradiation creep tests.[3,10] One of the characteristics of the embrittlement is its sensitivity to strain rate; lowering the strain rate results in a greater fractional reduction in ductility.[1,3,11,12] This particular study was to determine the degree of embrittlement of Hastelloy N at low stresses after various neutron exposures.

EXPERIMENTAL

The analyses of the two heats of Hastelloy N used in these investigations are given in Table I. The subsize specimens were irradiated at 50°C in the ORR to the neutron fluence levels shown in Table II. The postirradiation tests were performed in air in lever-arm creep machines shown in Fig. 1 or in a tensile machine described previously.[1] The 5065 heat was irradiated in the as-received condition whereas the 2477 heat was given a 1-hr anneal at 1036°C prior to irradiation. The relative movement of the specimen grips was automatically recorded and used as a measure of strain.

Four stress levels — 52,500, 39,800, 32,500, and 21,500 psi — were used and all tests were performed at 650°C.

POSTIRRADIATION CREEP AND STRESS-RUPTURE RESULTS

The creep and stress-rupture data for all tests are given in Table III. The stress-rupture strength and ductilities were in general reduced as the neutron fluence was increased. Heat 5065 was affected to a greater degree than was heat 2477.

Table I. Chemical Analyses of Alloys

Element	Content (wt %)	
	Heat 2477	Heat 5065
Mo	16.32	16.45
Cr	7.05	7.37
Fe	4.25	3.74
C	0.06	0.06
Si	0.015	0.58
Mn	0.04	0.55
Va		0.21
P		0.008
S	0.003	0.007
Al	0.06	0.01
Ti		0.01
B	0.0007	0.004
Co	0.14	0.08
Cu		0.01
Ni	Bal	Bal

Table II. Neutron Fluence for Irradiation Experiments

Experiment Designation	Neutron Fluence (neutrons/cm^2)	
	Thermal	E > 1 Mev
Φ_1	5×10^{16}	2.3×10^{15}
Φ_2	1.3×10^{18}	5.6×10^{16}
Φ_3	9.0×10^{18}	3.9×10^{17}
Φ_4	5.0×10^{10}	1.6×10^{18}
Φ_5	5×10^{20}	4×10^{20}

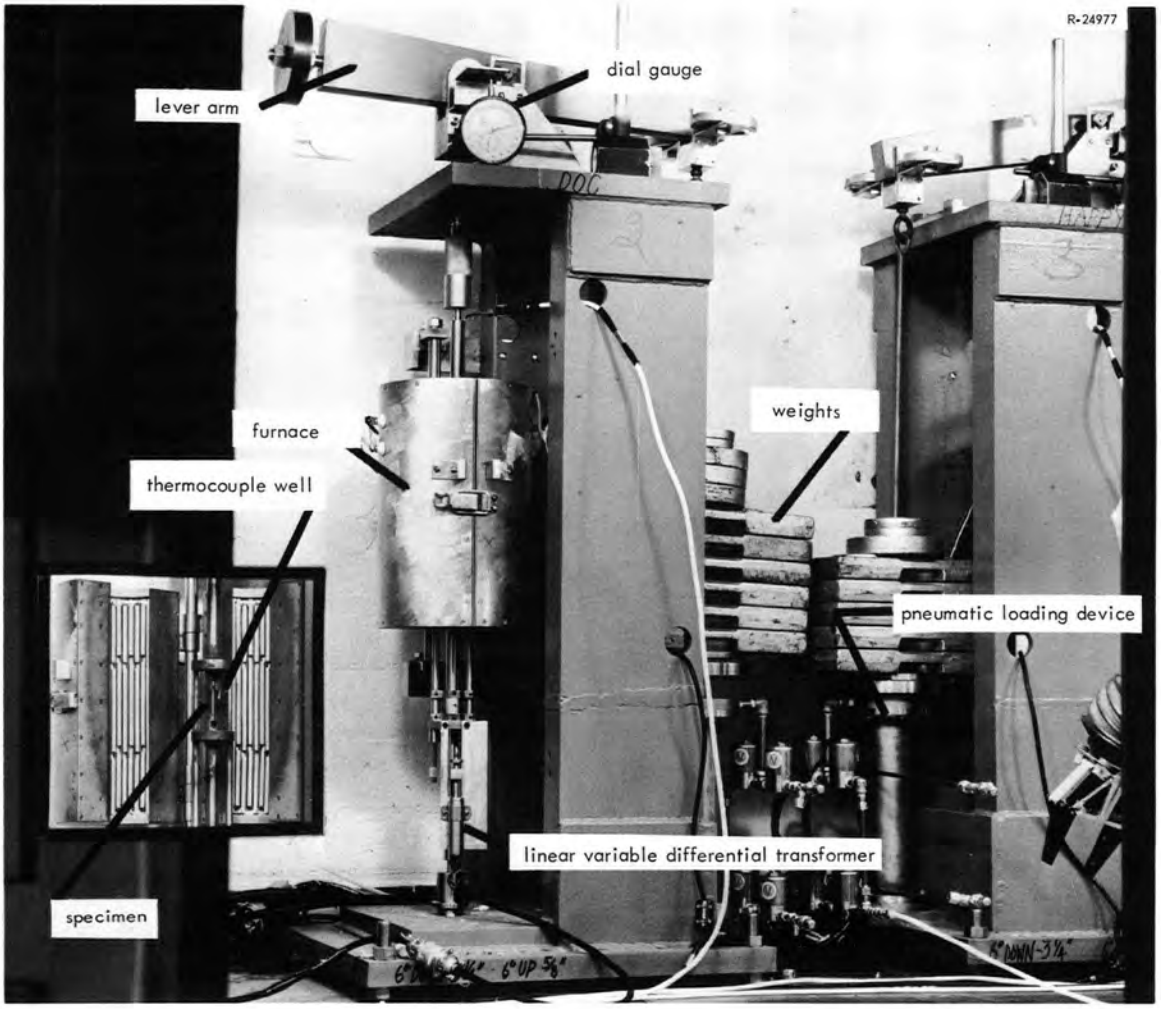

Fig. 1. Photograph of Postirradiation Creep Machine.

Table III. Postirradiation Creep and Stress-Rupture Results

Heat Number	Stress (10^3 psi)	Irradiation Fluence (neutrons/cm^2) Thermal	Fast	Time to Rupture (hr)	Total Elongation[a] (%)	Minimum Creep Rate (10^{-2}%/hr)
5065	52.5	5×10^{16}	2.3×10^{15}	21.2	2.6 (6.6)	9
		1.3×10^{18}	5.6×10^{16}	11.9	2.0 (6.0)	12
		9.0×10^{18}	3.9×10^{17}	5.1	3.4 (7.4)	19
		5.0×10^{19}	1.6×10^{18}	0.4	0.9 (4.9)	100
		5.0×10^{20}	4.0×10^{20}	0.9	0.6 (4.6)	68
	39.8	5.0×10^{16}	2.3×10^{15}	424.7	9.2	3.6
		1.3×10^{18}	5.6×10^{16}	147.0	5.7	3.2
		9.0×10^{18}	3.9×10^{17}	80.2	5.5	4.3
		5.0×10^{19}	1.6×10^{18}	23.5	1.2	3.5
		5.0×10^{20}	4.0×10^{20}	5.3	0.3	3.7
	32.5	5.0×10^{16}	2.3×10^{15}	686.7	6.7	0.7
		1.3×10^{18}	5.6×10^{16}	647.0	6.3	0.7
		9.0×10^{18}	3.9×10^{17}	232.2	2.5	0.9
		5.0×10^{19}	1.6×10^{18}	5.2 10.6	0.7 0.6	4.0 2.0
		5.0×10^{20}	4.0×10^{20}	8.0	0.4	3.0
	21.5	1.3×10^{18}	5.6×10^{16}	2373.7	2.6	0.07
		9.0×10^{18}	3.9×10^{17}	1603.0	2.7	0.15
		5.0×10^{19}	1.6×10^{18}	521.8	1.5	0.15
		5.0×10^{20}	4.0×10^{20}	312.0	0.8	0.15

Table III (continued)

Heat Number	Stress (10^3 psi)	Irradiation Fluence (neutrons/cm^2) Thermal	Fast	Time to Rupture (hr)	Total Elongation[a] (%)	Minimum Creep Rate (10^{-2}%/hr)
2477	52.5	5.0×10^{16}	2.3×10^{15}	70.7	2.8 (6.8)	2.6
		1.3×10^{18}	5.6×10^{16}	57.4	3.0 (7.0)	4.2
		9.0×10^{18}	3.9×10^{17}	30.4	4.6 (8.6)	11.5
		5.0×10^{19}	1.6×10^{18}	21.1	4.3 (8.3)	14.1
		5.0×10^{20}	4.0×10^{20}	19.9	4.7 (8.7)	13.8
	32.4	5.0×10^{16}	2.3×10^{15}	1070.7	3.9	0.4
		1.3×10^{18}	5.6×10^{16}	1525.7	6.3	0.4
		9.0×10^{18}	3.9×10^{17}	1425.1	11.2	0.7
		5.0×10^{19}	1.6×10^{18}	849.6	5.1	0.5
		5.0×10^{20}	4.0×10^{20}	515.2	3.4	0.5

[a]Total strain at 52,500-psi tests to include creep strain plus strain on loading are shown in parentheses (additional 4% tensile strain).

The stress-rupture properties of heat 5065 as a function of neutron fluence compared to those of the unirradiated alloy are shown in Fig. 2. These data suggest a stress dependence for the irradiation effect. That is, an effect is noted but only for tests above a threshold stress whose value is a function of the neutron fluence. This effect is similar to the one observed by Robertshaw et al.[10] for the postirradiation stress-rupture strength of Hastelloy X tested at 650 °C. This type of convergence was not observed by Pfeil and Harries[3] for the postirradiation tube-burst tests on type 316 stainless steel at 650 °C. Similarly, Robertshaw et al.[10] did not observe the convergence for the iron-base alloy A286 when testing at 650 °C.

The reduced rupture life appears to be primarily related to the degree of embrittlement. A comparison of creep curves (see Fig. 3) for testing at 21,500 psi at various neutron exposures indicates that the shorter life results from embrittlement and is not due to significant variations in the strain-time relationship. The slight increase in creep rate is well within that expected from experimental error. A few comments about the shape of the creep curve are in order.

Generally the third stage is either not present and the material fractures during secondary creep or the third stage is initiated earlier with only slight deformations occurring during an abbreviated third stage.

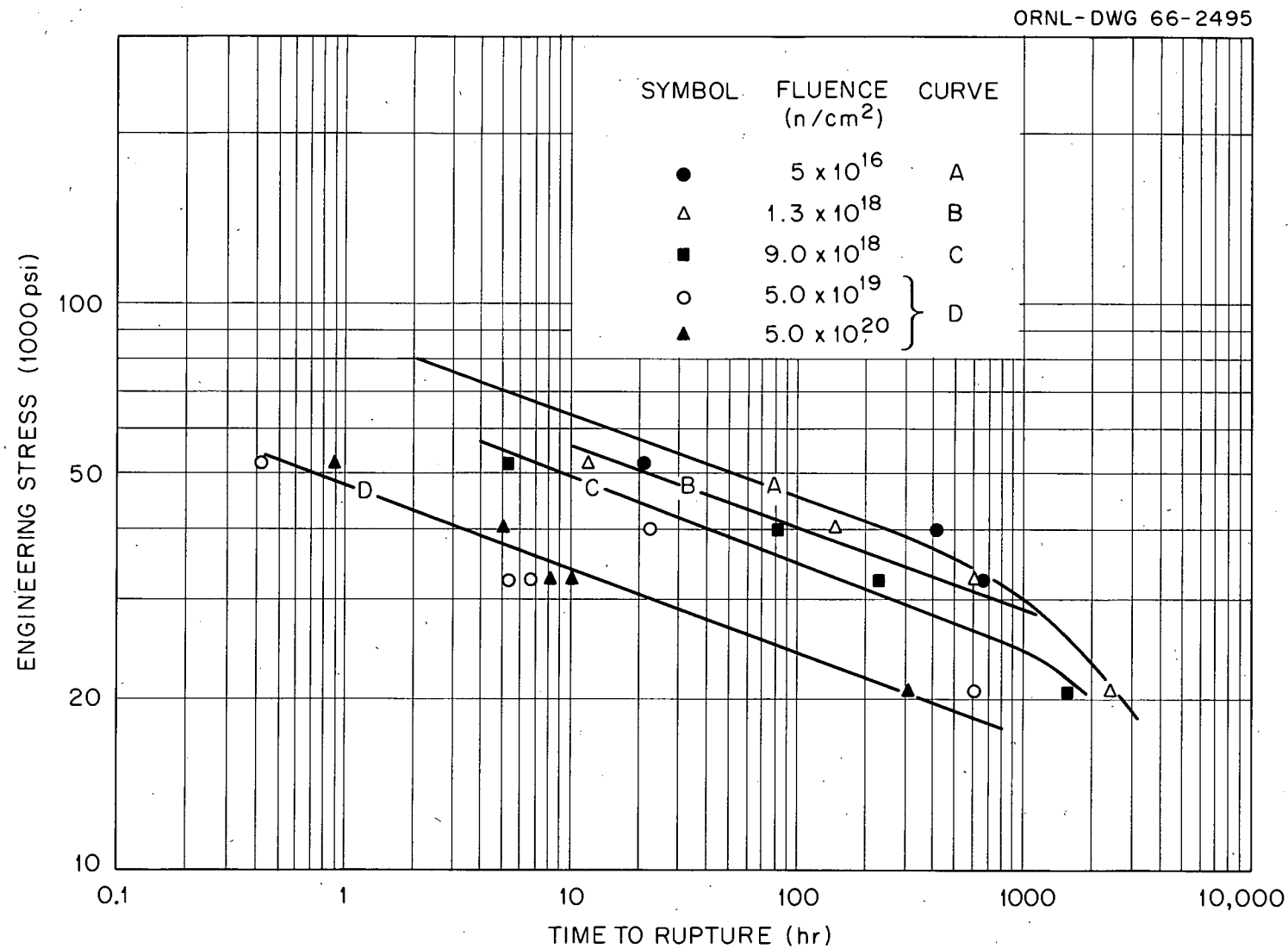

Fig. 2. Postirradiation Stress Rupture of Hastelloy N at 650°C.

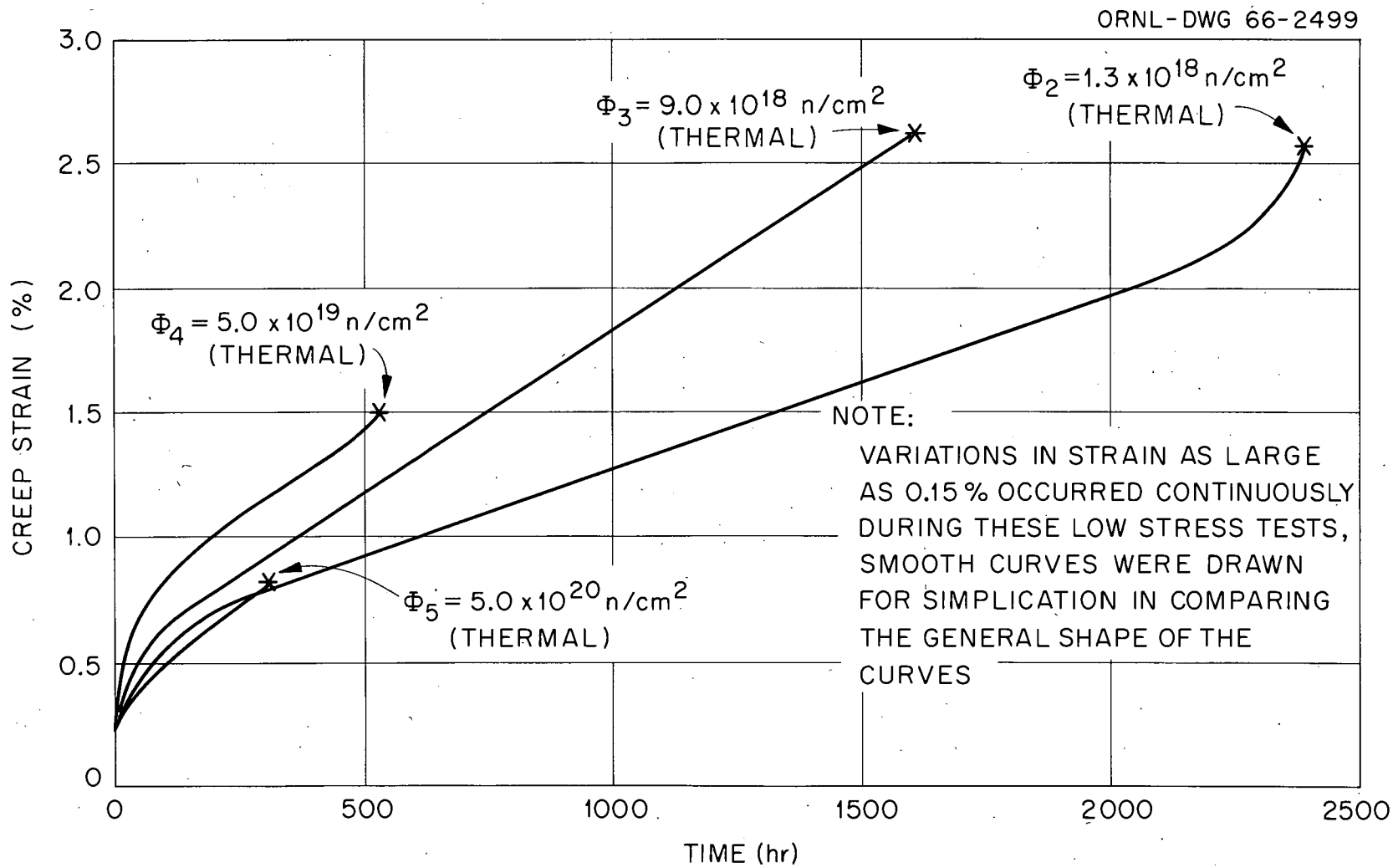

Fig. 3. Postirradiation Creep of Hastelloy N at 21,500 psi and 650°C.

The creep rates given in Table III can be easily misinterpreted. We have properly named them minimum creep rates, and some rates are an order of magnitude larger than the same heat irradiated to a lower fluence. Thus one could conclude from the data that irradiation damage has increased the creep rate; however, this is not believed the case. Assume, for example, that two irradiated samples have been deformed at identical conditions. One has been irradiated to a higher fluence than the other, but both fracture during the so-called second stage of creep at different rupture times. Although the stress-rupture life of these samples differs, both will have identical minimum and secondary creep rates. Now if we examine the data from a sample having a higher neutron fluence at these same test conditions, we find the fracture occurs during primary creep and the minimum creep rate of the sample is much larger than the minimum or secondary creep rate of the previous samples. However, the strain-time relationship has not been changed. We believe that this is indeed the explanation for the creep rate data in Table III and another set of creep curves for heat 5065 are given in Fig. 4 for support of this concept.

The ductilities of the heat 5065 for deformations in a short-time tensile test are given in Table IV. These data along with those given in Table III are used to examine the relationship between rupture ductility and strain rate. Figure 5 shows

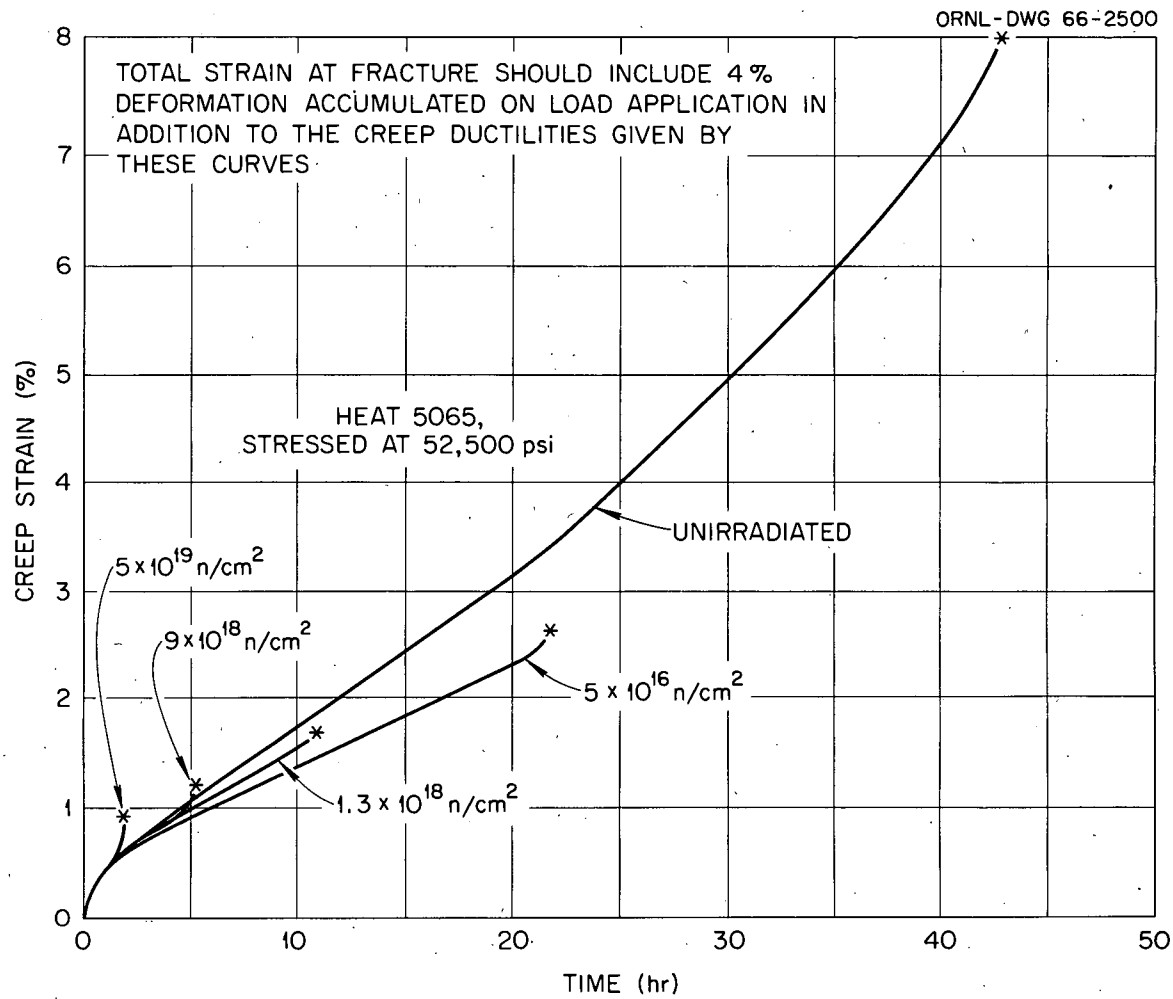

Fig. 4. Postirradiation Creep of Hastelloy N at 52,500 psi and 650°C.

Table IV. Ductilities of Hastelloy N in Short-Time Tensile Tests at 650 °C

Thermal Neutron Fluence (neutrons/cm^2)	Total Elongation[a] (%)
0	35.1
1.3×10^{18}	30.3
9.0×10^{18}	31.1
5.0×10^{19}	23.3

[a]Measured at a strain rate of 2%/min.

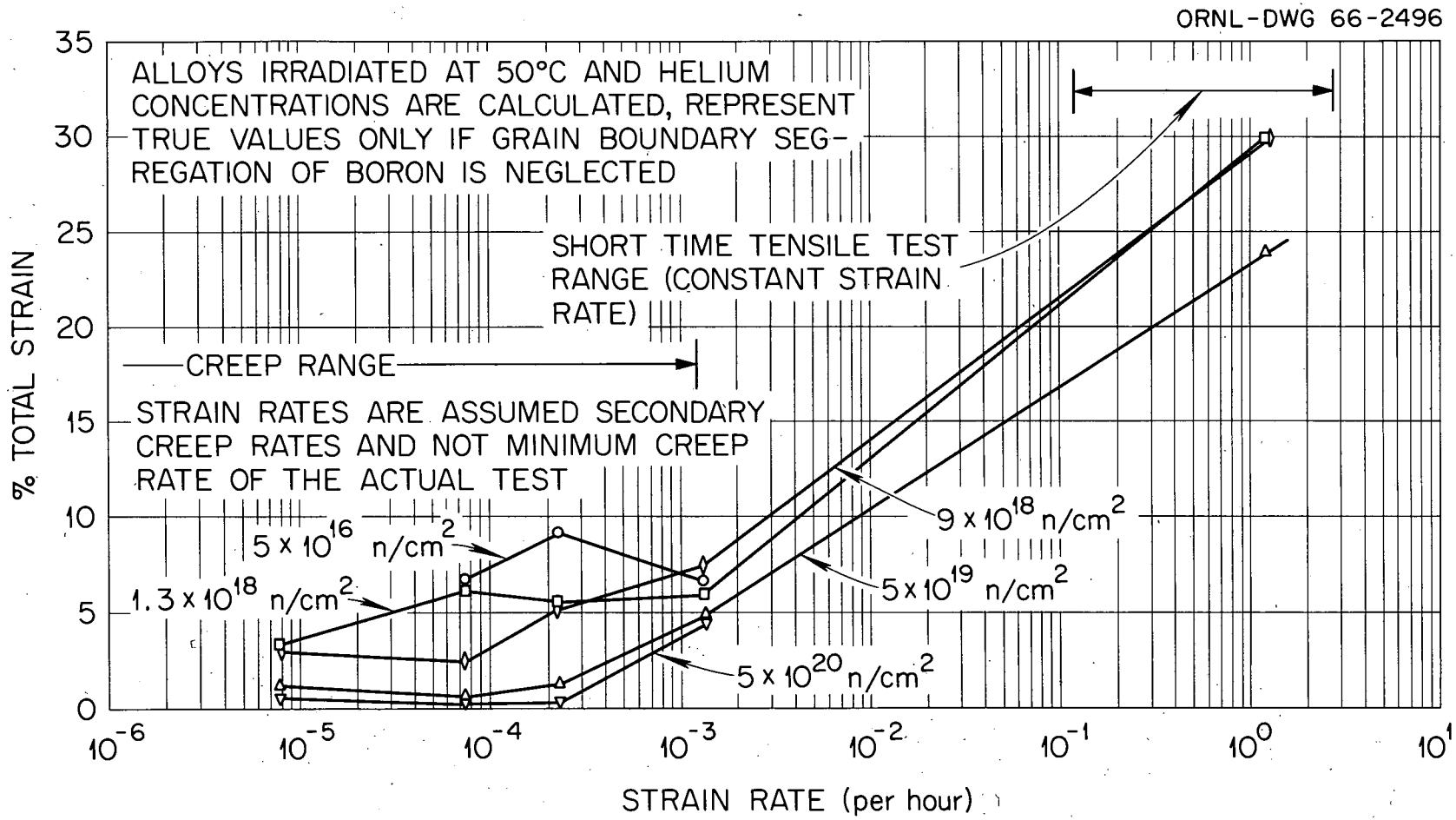

Fig. 5. Strain-Rate Sensitivity of Irradiated Hastelloy N Embrittlement.

the markedly reduced ductilities at the lower strain rates. The lowest ductility at a given strain rate is associated with the highest neutron exposure. But the ductilities for all the low-stress tests are low, a phenomenon consistent with the behavior of many unirradiated alloys.

Photomicrographs of the fractured samples are given in Figs. 6, 7, and 8. These photographs indicate a decreasing resistance to the propagation of grain-boundary cracks. The samples subjected to the lowest neutron fluence are the most ductile and have the greatest number of wedge-type fractures. The photomicrographs given in these figures show no change in microstructure at magnifications of 500×.

The general behavior of the 2477 heat was similar to heat 5065 but the alloy was less affected for a given fluence and stress level. There are several differences between the two heats. The boron content in the 5065 heat was 37 ppm, compared with 7 ppm by weight for heat 2477. The significance of other chemistry variations (Table I) between the two heats is not known. Heat 5065 was an air-melted heat whose fabrication history was probably different from that of vacuum-melted heat 2477. Although the grain sizes of the heats are comparable (as seen from Fig. 9), a more duplex structure is noted in heat 2477. Finally, heat 2477 was given a solution anneal at 1175°C prior to irradiation, whereas the 5065 was tested in the

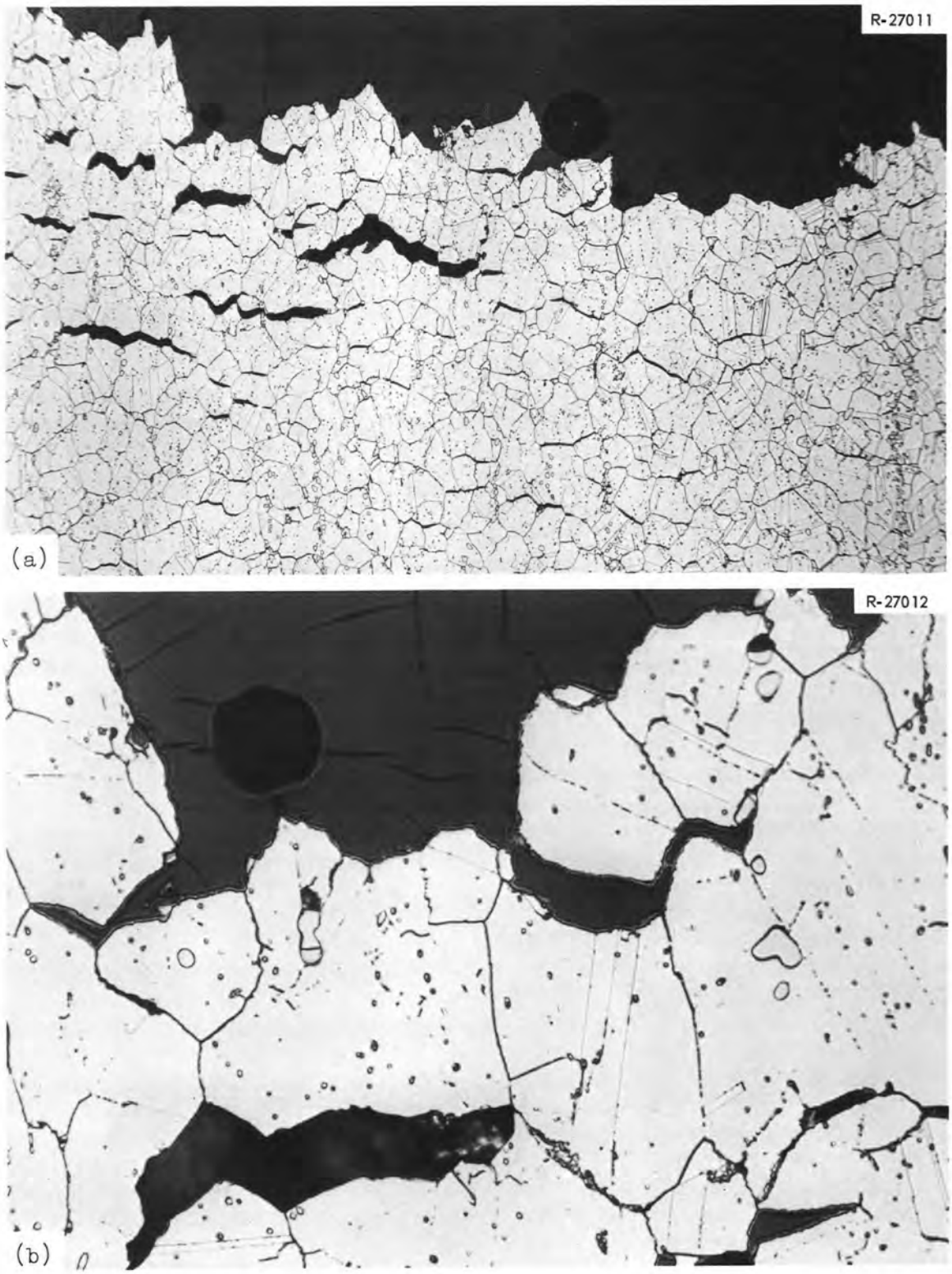

Fig. 6. Microstructure of Irradiated Hastelloy N (Heat 5065) after Creep Test at 32,400 psi and 650°C. Rupture at 647 hr with 6.3% strain. (a) 100×; (b) 500×. Thermal neutron fluence – 1.3×10^{18} neutrons/cm^2.

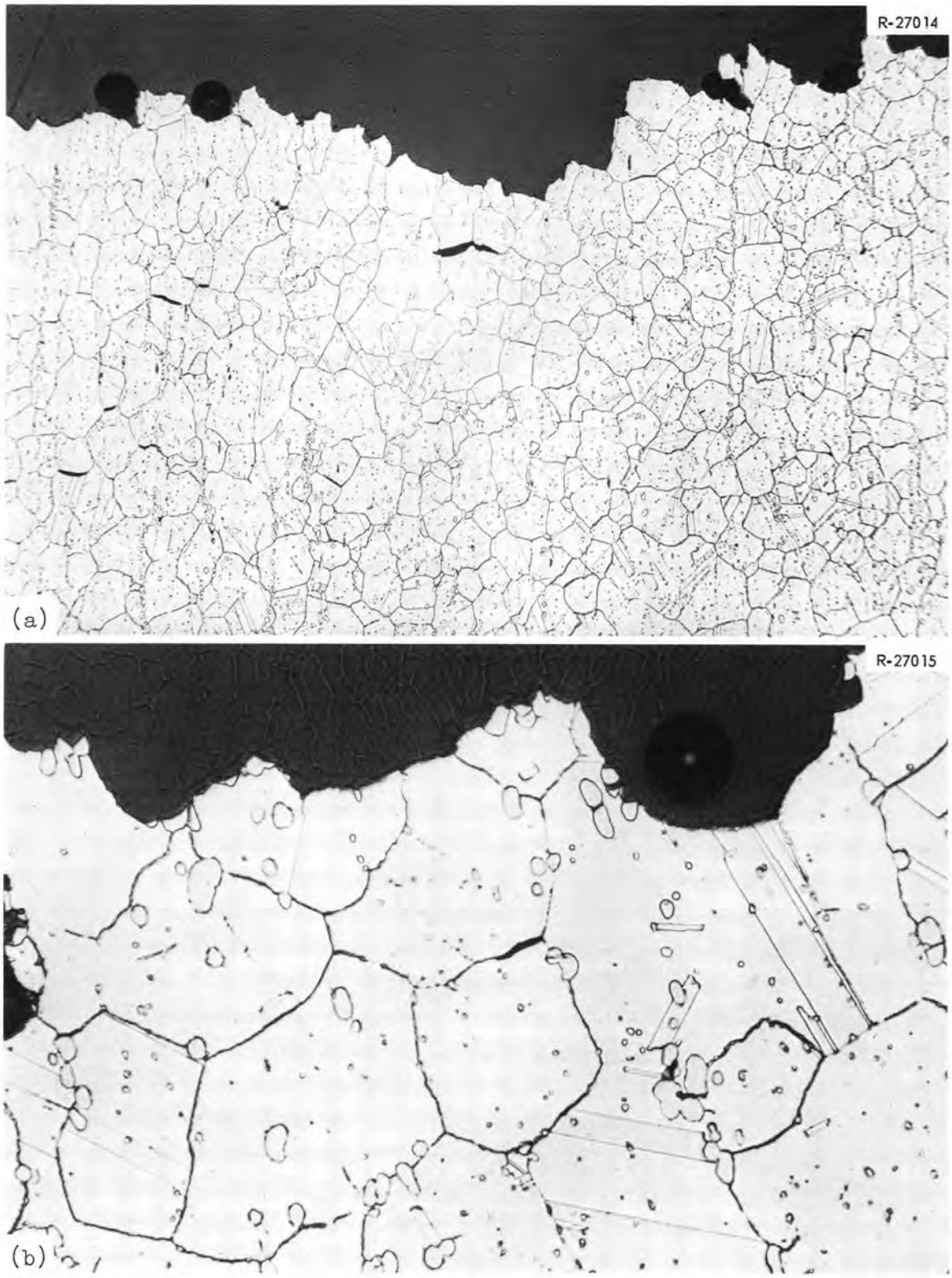

Fig. 7. Microstructure of Irradiated Hastelloy N (Heat 5065) after Rupture at 232.2 hr and 2.5% Strain for a Stress of 32,400 psi. (a) 100×; (b) 500×. Thermal neutron fluence – 9×10^{18} neutrons/cm^2.

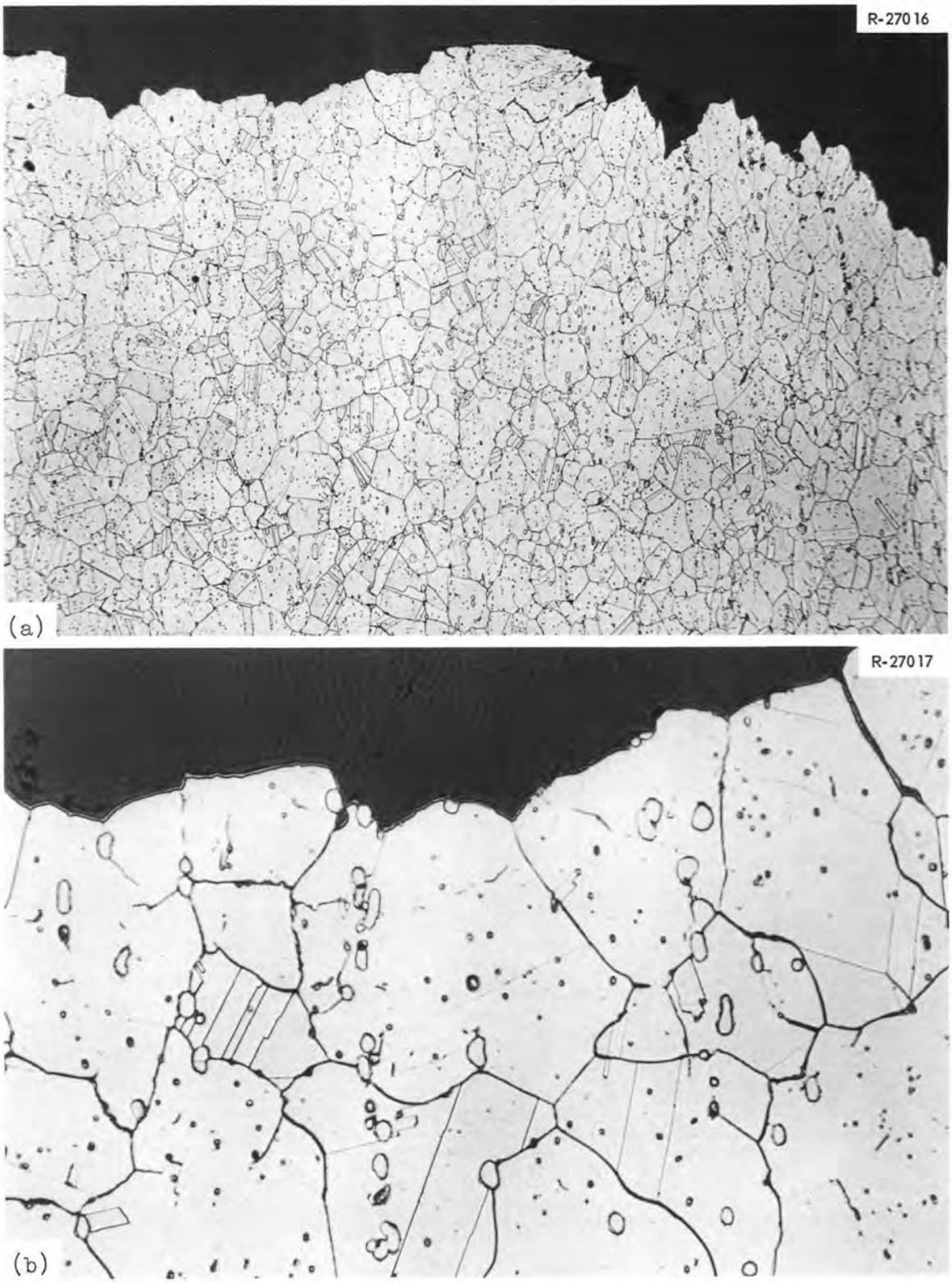

Fig. 8. Microstructure of Irradiated Hastelloy N (Heat 5065) after Creep at 32,400 psi and 650 °C. Fracture occurred at 8.0 hr and 0.42% strain. (a) 100×; (b) 500×. Thermal neutron fluence – 5×10^{20} neutrons/cm^2.

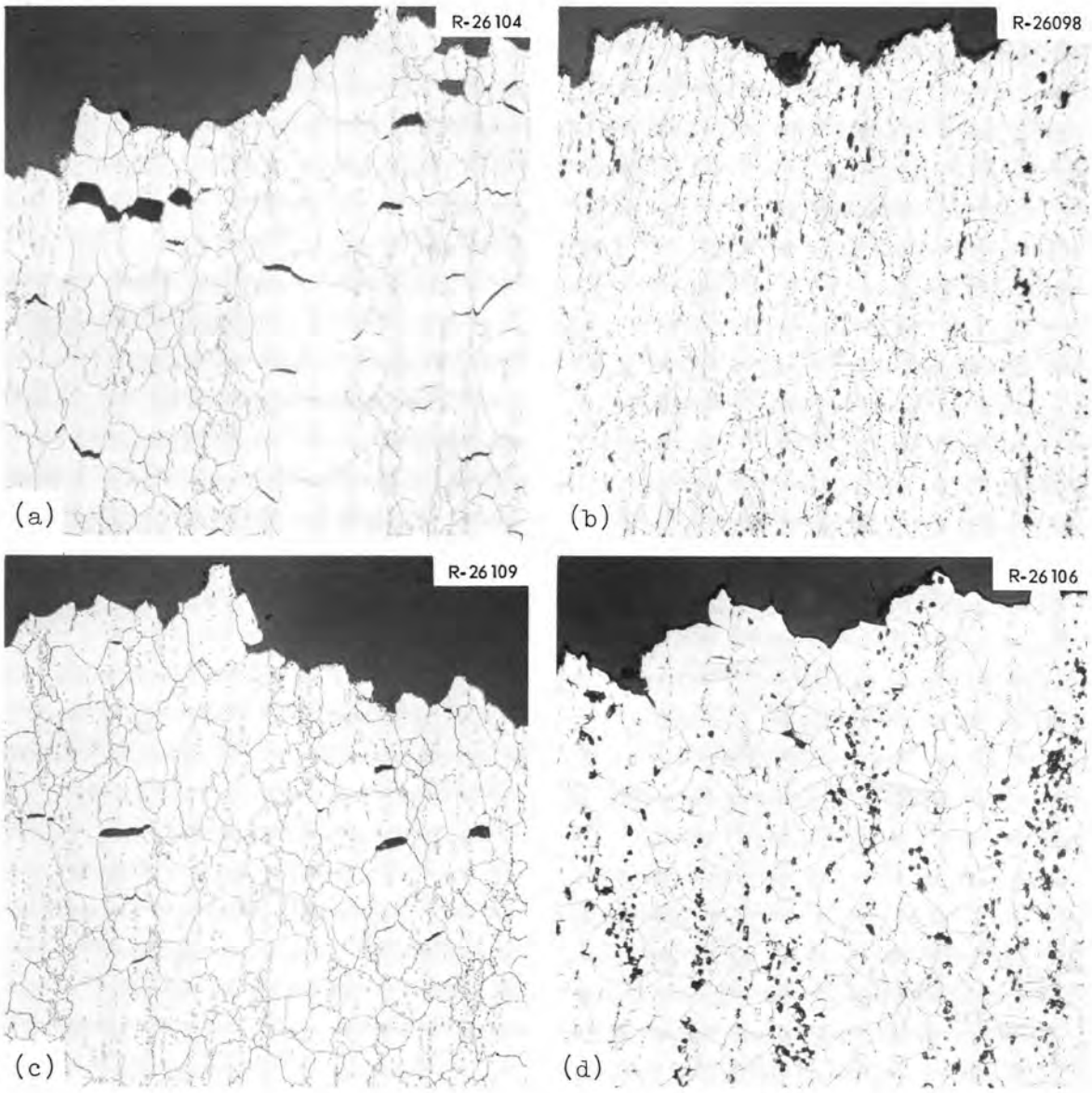

Fig. 9. Comparison of Fractures in Heats 2477 and 5065 Irradiated to 5×10^{19} neutrons/cm^2. (a) Heat 2477 stressed at 52,600 psi and fractured in 21.1 hr at 4.3% strain. (b) Heat 5065 stressed at 52,600 psi and fractured in 0.4 hr at 0.9% strain. (c) Heat 2477 stressed at 32,400 psi and fractured in 849.6 hr at 5.1% strain. (d) Heat 5065 stressed at 32,400 psi and fractured in 5.2 hr at 0.7% strain. 100×.

as-received condition. It is not clear which (if any) of the variations cited above are the most important. The magnitude of boron content would be important, of course, if the distribution of boron were the same in the two heats. The ductility of both heats as a function of helium content is given in Fig. 10. The ductility of heat 5065 decreases with increasing helium content, and the ductility of heat 2477 decreases at the higher fluence levels but goes through a maximum at approximately 10^{-7} atom fraction of helium. It is possible that lower ductility observed for heat 2477 containing less than 10^{-7} atom fraction of helium is associated with an aging phenomenon that occurs in these longer creep tests. Also the helium content given in Fig. 10 was calculated with the unlikely assumption that all the helium atoms were homogeneously dispersed within the grains. But since the degree of segregation to the grain boundary is not known, such an assumption is valid for the comparison of the two alloys. Furthermore, it is observed that for a given neutron fluence and creep condition, more grain-boundary cracks were found in heat 2477 than 5065. Thus from Fig. 8 one can suggest that the resistance to the propagation of grain-boundary cracks is higher in heat 2477 compared with heat 5065.

The mechanism for helium embrittlement could be related to helium bubbles serving as grain-boundary crack nuclei. In creep, the role of bubbles as crack nuclei can be described in terms

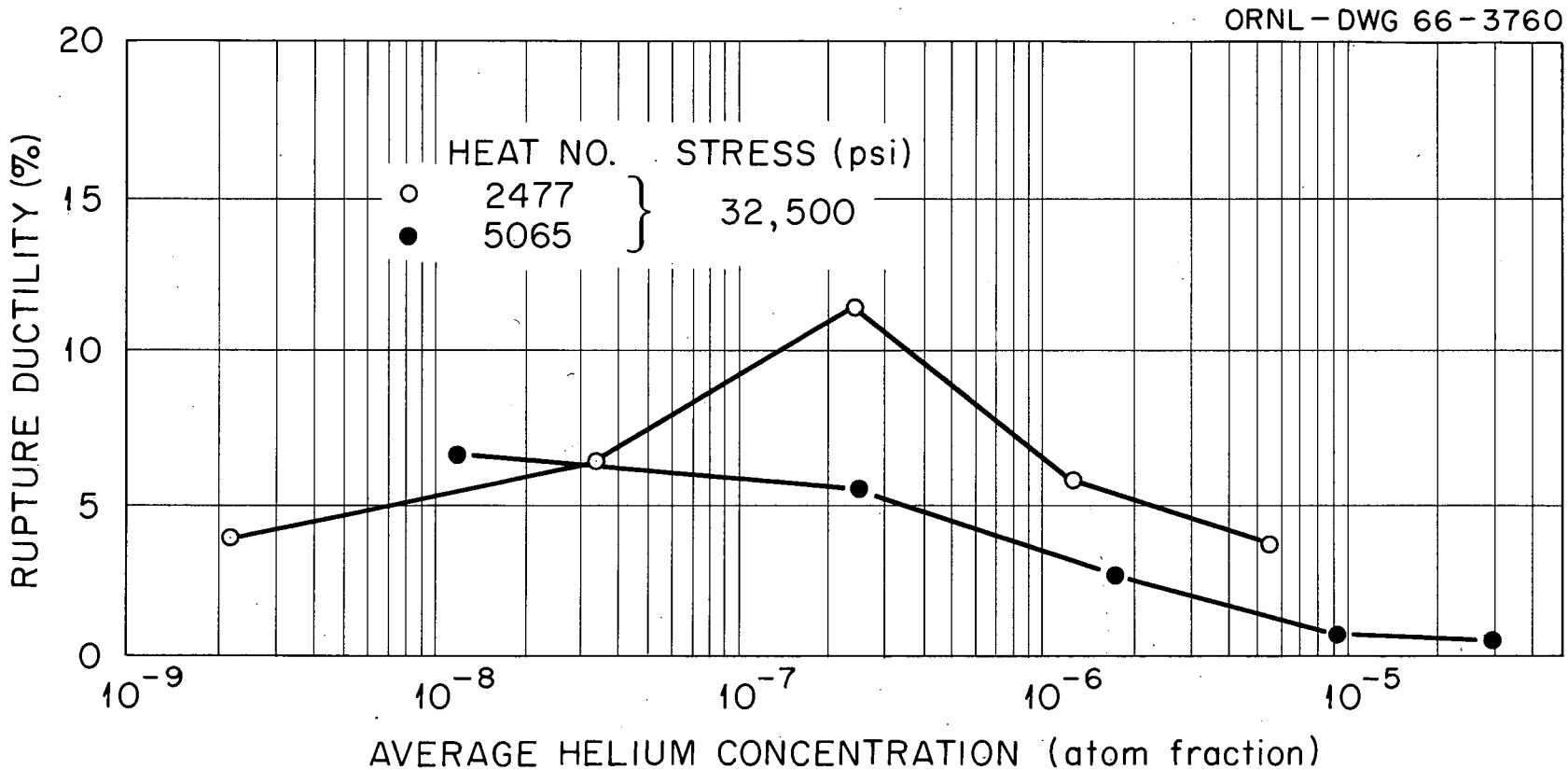

Fig. 10. Rupture Ductility of Irradiated Hastelloy N at 650°C.

of an existing theory proposed for the cavitation type of intergranular fracture.

It is proposed that helium bubbles serve as crack nuclei because they are cavities that can grow large enough for vacancies to migrate into them at the applied stress level. That is, there is a critical size of cavity below which the cavity does not enlarge at a given stress level by a simple vacancy migration or addition process. The converging postirradiation stress-rupture data can be explained by such a relationship. The critical size of bubbles can be calculated via the energy criterion method. This is given in detail by McLean[13] but can be approximated as follows. The critical radius, r_o, is inversely proportional to the stress, σ. Therefore,

$$\sigma \propto \frac{1}{r_o} .$$

Assuming the bubbles are approximately constant in number and are spherical, then $r_o^3 \propto C$, where C is the concentration of helium. Combining these we get

$$\sigma \propto C^{-1/3} .$$

We can also check this relationship by appropriate analysis of our stress-rupture data. Figure 11 shows a linear relationship between the log time to rupture and the log of the reciprocal of

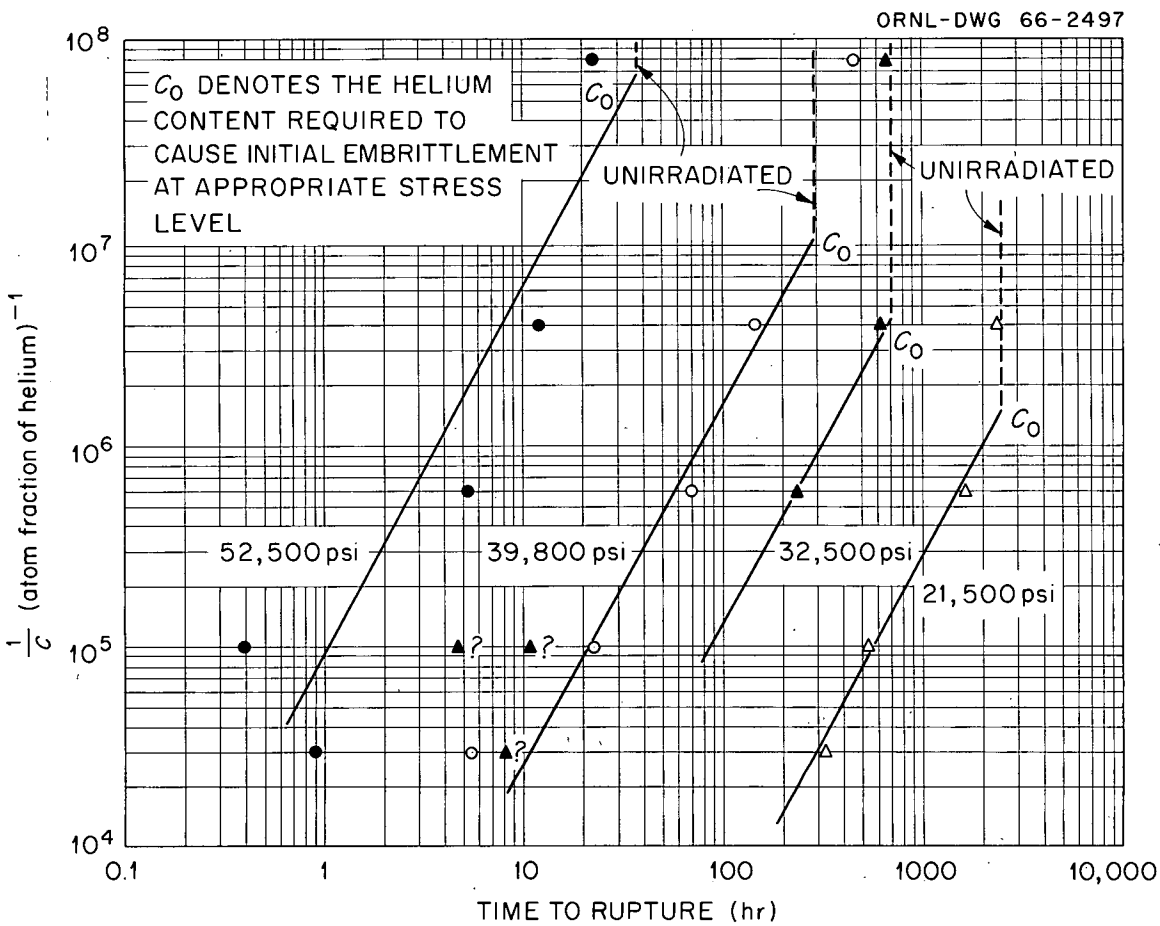

Fig. 11. Relationship Between Calculated Helium Content and Stress Rupture.

helium concentration. From this plot and unirradiated stress-rupture data one can determine the amount of helium necessary to initiate embrittlement. The critical helium content is related to the stress as predicted by the above equations, as shown in Fig. 12. The agreement between theory and experiment has been shown with the two important assumptions. The total number of equally spaced bubbles does not change significantly with fluence, and the stress concentration at boundaries is proportional to the applied stress. These assumptions are probably valid for the range of helium contents investigated.

A theory for stress rupture based on the growth of grain-boundary voids under stress has been proposed by Hull and Rimmer.[14] This relationship in exact solution can be found in the literature. But Hull and Rimmer found a decrease in the intervoid distance with increase in stress of tests with copper. A decrease of a factor of 2 was found for an increase from 4000 to 6000 psi. In contrast, Oliver and Girifalco[15] assumed a fixed number of void nuclei and a Gaussian distribution for void nuclei size. Oliver and Girifalco assumed that the time to rupture is reached when a critical fraction F_c of grain-boundary area A contains n voids of mean radius F_c. Their relationship between time to rupture and strain rate is given by

$$t_r = X\left(\frac{F_c A}{n\pi V k \dot{\epsilon} D}\right)^{1/2},$$

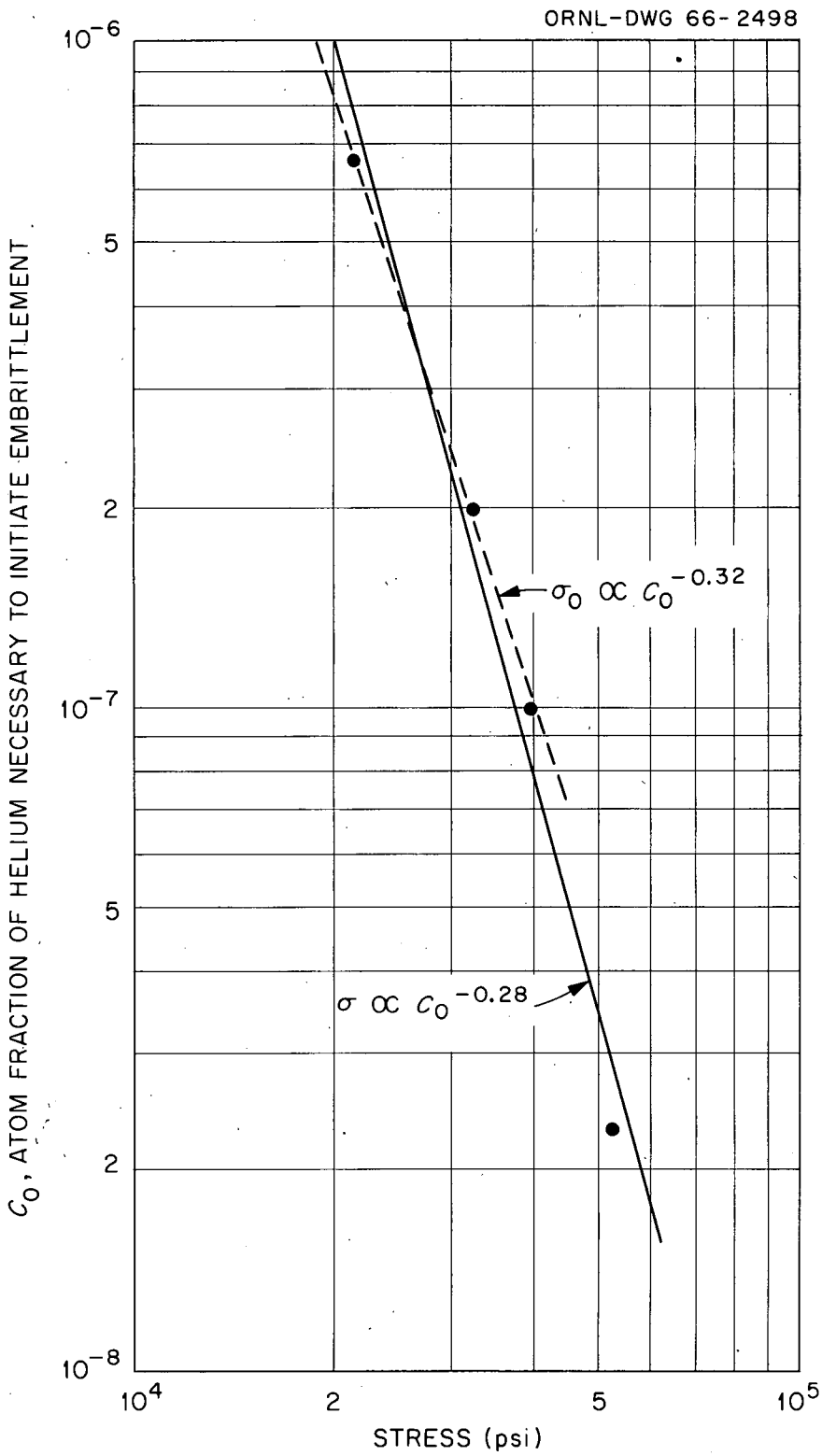

Fig. 12. Critical Helium Content as a Function of Creep Stress.

where V is the volume of defect-producing void growth, k and x are constants, $\dot{\epsilon}$ is the strain rate, and D is the bulk diffusion coefficient for the defect. Let us consider that irradiation affects the quantity within the parentheses. If so, the time to rupture is proportional to some irradiation parameter to the one-half power. It is important to note that the slope of the critical fraction of helium and time to rupture, given in Fig. 11, is approximately 0.55. This further agreement between theory and experiment provides more evidence to support an irradiation embrittlement mechanism based on intergranular fracture and helium.

CONCLUSIONS AND SUMMARY

The postirradiation stress-rupture properties of Hastelloy N are highly sensitive to neutron fluence. The reduction in rupture life is more severe at the higher fluence levels. At a given neutron fluence there exists a stress level below which no embrittlement is observed. This threshold stress level is approximately related to the neutron fluence, or possibly the helium content, to the one-third power. This observation is consistent with the concept of helium bubbles serving as crack nuclei whose critical diameter is related to stress. The reduction in stress-rupture life is due to a reduction in ductility with the absolute value of ductility being lower at the lower strain rate tests. The rate of decrease in time to rupture with helium content corresponds to a

power low of one-half predicted by the relationship given by Oliver and Girifalco[15] for stress rupture based on the growth of voids. No consistent or significant variations in the stress-strain relationship were observed. The reduction in stress-rupture life and in many cases the ductility is accompanied by a lower density of grain-boundary cracks of a size visible in the optical microscope. This evidence supports the hypothesis for elevated-temperature irradiation embrittlement being related to an effect of helium on the process of intergranular fracture.

ACKNOWLEDGMENTS

The authors wish to acknowledge the assistance during the investigation of J. W. Woods, V. R. Bullington, D. G. Gates, E. H. Lee, Z. R. McNutt, and in particular K. W. Boling.

REFERENCES

1. W. R. Martin and J. R. Weir, Nucl. Appl. 1, 160 (1965).

2. N. E. Hinkle, Am. Soc. Testing Mater. Spec. Tech. Publ. No. 341, 344 (1963).

3. P.C.L. Pfeil and D. R. Harries, Am. Soc. Testing Mater. Spec. Tech. Publ. No. 380, 251 (1965).

4. P.R.B. Higgins and A. C. Roberts, Nature 206, No. 4990, 1250 (1965).

5. H. Alter and C. E. Weber, J. Nucl. Mater. 16, 68 (1965).

6. H. Bush, J. Moteff, and J. R. Weir, Radiation Damage in Fast Reactor Components, p. 170 in "Fast Reactor Technology," American Nuclear Society Report No. ANS-100 (1965).

7. N. A. Hughes and J. Coley, J. Nucl. Mater. 10, 60 (1963).

8. W. R. Martin and J. R. Weir, Nature 202, No. 4936, 997 (1964).

9. J. T. Venard and J. R. Weir, Am. Soc. Testing Mater. Spec. Tech. Publ. No. 380, 269 (1965).

10. F. C. Robertshaw, J. Moteff, F. D. Kingsbury, and M. A. Pugnaz, Am. Soc. Testing Mater. Spec. Tech. Publ. No. 341, 372 (1963).

11. W. R. Martin and J. R. Weir, Am. Soc. Testing Mater. Spec. Tech. Publ. No. 380, 251 (1965).

12. G. H. Broomfield, "The Effects of Strain Rate, Neutron Dose, and Irradiation Temperature on the Tensile Properties of Nimonic PE16," AERE-R-4982, United Kingdom Atomic Energy Agency (July 1965).

13. D. McLean, Mechanical Properties of Metals, p. 334, John Wiley and Sons, New York (1962).

14. D. Hull and D. E. Rimmer, Phil. Mag. 4, 673 (1959).

15. P. R. Oliver and L. A. Girifalco, Acta Met. 10, 765 (1962).

INTERNAL DISTRIBUTION

1–2. Central Research Library
3. Reactor Division Library
4. ORNL – Y-12 Technical Library Document Reference Section
5–24. Laboratory Records Department
25. Laboratory Records, ORNL R.C.
26. ORNL Patent Office
27. R. G. Berggren
28. G. E. Boyd
29. R. B. Briggs
30. J. E. Cunningham
31. W. W. Davis
32. D. A. Douglas, Jr.
33. J. H Frye, Jr.
34. W. O. Harms
35–37. M. R. Hill
38. C. F. Leitten, Jr.
39. H. G. MacPherson
40. H. E. McCoy, Jr.
41–50. W. R. Martin
51. E. C. Miller
52. P. Patriarca
53. G. M. Slaughter
54. D. B. Trauger
55. J. T. Venard
56. M. S. Wechsler
57. A. M. Weinberg
58. J. R. Weir
59–78. G. D. Whitman
79. J. W. Woods

EXTERNAL DISTRIBUTION

80. C. M. Adams, Jr., Massachusetts Institute of Technology
81. J. Brunhouse, Aerojet, General Nucleonics
82. D. B. Coburn, General Atomic
83. F. Comprelli, General Electric, San Jose
84–85. D. F. Cope, AEC, Oak Ridge Operations
86. P. Fortescue, General Atomic
87. J. L. Gregg, Bard Hall, Cornell University
88. J. E. Irwin, General Electric, Hanford
89–90. V. B. Lawson, Atomic Energy of Canada Ltd., Chalk River
91. J. Moteff, General Electric, NMPO, Cincinnati
92. R. E. Schreiber, E. I. Du Pont De Nemours Company, Savannah River Laboratory
93. F. Shober, Battelle Memorial Institute
94. A. A. Shoudy, Atomic Power Development Associates, Inc.
95–97. J. M. Simmons, AEC, Washington
98. E. E. Stansbury, University of Tennessee
99. J. C. Tobin, General Electric, Hanford
100. S. R. Vandenberg, General Electric, San Jose
101. Division of Research and Development, AEC, Oak Ridge Operations
102–116. Division of Technical Information Extension